Dressed Rabi Oscillation in a Crystalline Organic Radical

C. Blake Wilson,[1,2] Devin T. Edwards,[1,2] Jessica A. Clayton,[1,2] Songi Han,[2,3] and Mark S. Sherwin[1,2,*]
[1]Department of Physics, University of California, Santa Barbara, Santa Barbara, California, USA
[2]Institute for Terahertz Science and Technology, University of California, Santa Barbara, Santa Barbara, California, USA
[3]Department of Chemistry and Biochemistry, University of California, Santa Barbara, Santa Barbara, California, USA

(Received 16 April 2019; revised manuscript received 4 October 2019; published 29 January 2020)

Free electron laser-powered pulsed electron paramagnetic resonance experiments performed at 240 GHz/8.56 T on the crystalline organic radical 1,3-bisdiphenylene-2-phenylallyl reveal a tip-angle dependent resonant frequency. Frequency shifts as large as 11 MHz (45 ppm) are observed during a single Rabi oscillation. We attribute the frequency shifts to a "dressing" of the nutation by spin-spin interactions. A nonlinear semiclassical model which includes a temperature- and sample-geometry-dependent demagnetizing field reproduces experimental results. Because experiments are performed without a cavity, radiation damping, the most common nonlinear interaction in magnetic resonance, is negligible in our experiments.

DOI: 10.1103/PhysRevLett.124.047201

Understanding the magnetic properties of systems with unpaired electron spins is at the heart of much of modern condensed matter physics. Over the past decades, extensive efforts have focused on understanding systems at thermal equilibrium. As a result, ordered ground states such as the ferromagnet and antiferromagnet (AFM) are now well understood. Much current research on magnetism in thermal equilibrium focuses on the search for more exotic, highly entangled ground states such as quantum spin liquids in frustrated magnets [1–8]. The behavior of large numbers of interacting spins far from equilibrium, however, remains challenging to study despite intense theoretical [9] and experimental investigations [10].

Crystalline organic radicals—crystals composed of organic molecules that each contain an unpaired electron spin—are promising candidates for hosting interesting phases of strongly interacting spins driven far from equilibrium. Spins are sufficiently close to each other that the dominant interaction is exchange, but, because of small spin-orbit coupling, spins are sufficiently isolated from the lattice that a nonequilibrium spin state decays much more slowly than the timescales associated with spin-spin interactions.

BDPA (1,3-bisdiphenylene-2-phenylallyl), also known as the Koelsch radical, is an organic spin-1/2 radical that has been the subject of much study [11–15] and is widely used as a standard sample in electron paramagnetic resonance (EPR) [16–18] and as a polarizing agent in dynamic nuclear polarization enhanced nuclear magnetic resonance (NMR) experiments [19,20]. Crystallized 1:1 complexes of BDPA with benzene (BDPA-Bz, $C_{39}H_{27}$) are well described by a quasi-one-dimensional Heisenberg AFM linear chain model, with an exchange integral $J/k_B = -4.4$ K along the chain [11,14], isosceles type spin frustration [12], and the onset of antiferromagnetic order at 1.695 K [11]. Well above the ordering temperature, the exchange interaction remains important. Thermal fluctuations in the exchange fields narrow the EPR line to a value much smaller than one would expect based on dipole-dipole interactions [21,22].

In this Letter, we report the observation of a novel dynamical phenomenon we call dressed Rabi oscillations. Rabi oscillations occur when an ensemble of spins is placed in a static magnetic field B_0 and driven by a transverse magnetic field B_1 oscillating near the Larmor frequency $\omega_0 = g\mu_B B_0/\hbar$. If the Rabi frequency $\omega_1 = g\mu_B B_1/\hbar$ is larger than the linewidth Γ of the magnetic resonance, the spin ensemble undergoes nutation and the direction of the spin ensemble magnetization vector traces out circles on the surface of the Bloch sphere in the rotating frame. We report on Rabi oscillation experiments performed on grains of crystalline BDPA with $\Gamma/2\pi = 4$–6 MHz at $B_0 = 8.56$ T, where the electron spin Larmor frequency is 240 GHz, driven by pulses of resonant radiation from the University of California, Santa Barbara (UCSB) mm-wave free electron laser (FEL) with Rabi frequencies ω_1 as large as 25 MHz. We find that Rabi oscillations are dressed by spin-spin interactions and exhibit nonlinear dynamics which we model semiclassically with a Bloch equation modified to include the effects of sample magnetization.

Individual BDPA-Bz grains were mounted on a silver-coated mirror and placed at the end of a corrugated waveguide which tapers to a diameter of 5 mm, then loaded into the center of a tunable (0 to 12.5 T) superconducting magnet. Each grain was ~300 to ~500 μm across, significantly smaller than the 1.25 mm wavelength 240 GHz radiation. Linearly polarized 240 GHz radiation generated by the UCSB mm-FEL in "long" pulses of 1 to 3 μs were "sliced" into excitation pulses of well-defined duration by light-activated silicon switches [23]. The silvered mirror below the

BDPA-Bz reflected both the linearly polarized excitation pulse and the circularly polarized EPR signal to a superheterodyne receiver. A light-activated silicon isolation switch placed before the receiver was turned on only after the excitation pulse had passed. For short excitation pulses < 40 ns, the FEL cavity dump coupler [24] was used to boost the excitation pulse power. When longer excitation pulses were required, the cavity dump coupler was not activated. Single-frequency operation of the FEL was achieved through injection locking [25]. For details of the FEL-EPR spectrometer, see [26–28].

Figure 1(a) shows the response of a single BDPA-Bz grain placed in a 8.56 T field to a 2 ns long, resonant excitation pulse with a Rabi frequency $\omega_1/2\pi = 25$ MHz. The short, resonant pulse tips the sample magnetization away from thermal equilibrium, which subsequently precesses at 240 GHz and emits circularly polarized magnetic dipole radiation proportional to the magnetization's projection onto the transverse plane. After a ~75 ns delay, the silicon isolation switch activates and a free induction decay (FID) is acquired by the receiver, mixed down to an intermediate frequency (IF = 500 MHz), and digitized. The complex FID signal is then Fourier transformed to extract the Fourier transform-EPR (FT-EPR) line shape [Fig. 1(b)]. Figure 1(c) shows the integrated FT-EPR power spectrum as a function of pulse length. As the pulse length increases, the magnetization rotates further in the Bloch sphere, undergoing Rabi oscillations [29]. At the first signal maximum, occurring for a 10 ns excitation pulse duration, the magnetization has rotated by $\pi/2$, while at the first minimum, occurring at around 20 ns, the magnetization has nominally been inverted. However, the fact that this minimum does not correspond to an integrated FT-EPR intensity near zero indicates inversion is far from complete.

Analysis of the FT-EPR signal in frequency space reveals the frequency of the FID, as measured by the FT-EPR signal, changes as a function of pulse length [Fig. 1(d)]. This indicates that the EPR frequency ω_0, typically given by the Larmor condition $\omega_L = \gamma B$ where $\gamma = g\mu_B/\hbar$, changes as a function of pulse length, a situation unexpected in conventional EPR experiments. The driven change in EPR frequency ω_0 can be attributed to the mean field exerted on one spin by all the other spins in the sample. The dressed Rabi oscillation phase can be modeled in a mean-field sense by modifying the semiclassical Bloch equations to include the demagnetizing field H_M of the BDPA-Bz grain itself, by analogy to ferromagnetic resonance (FMR) [30]. For an ellipsoid, $\mathbf{H}_M = -N \cdot \mathbf{M}$ where $\mathbf{M}$ is the magnetization and N is the demagnetization tensor [31]. Writing the total magnetic field $\mathbf{B} = \mu_0(\mathbf{H}_0 + \mathbf{H}_M + \mathbf{M})$, the Bloch equations in the absence of an excitation pulse and neglecting relaxation become

$$\frac{d}{dt}\mathbf{M} = \gamma\mathbf{M} \times \mu_0(\mathbf{H}_0 - N \cdot \mathbf{M}), \tag{1}$$

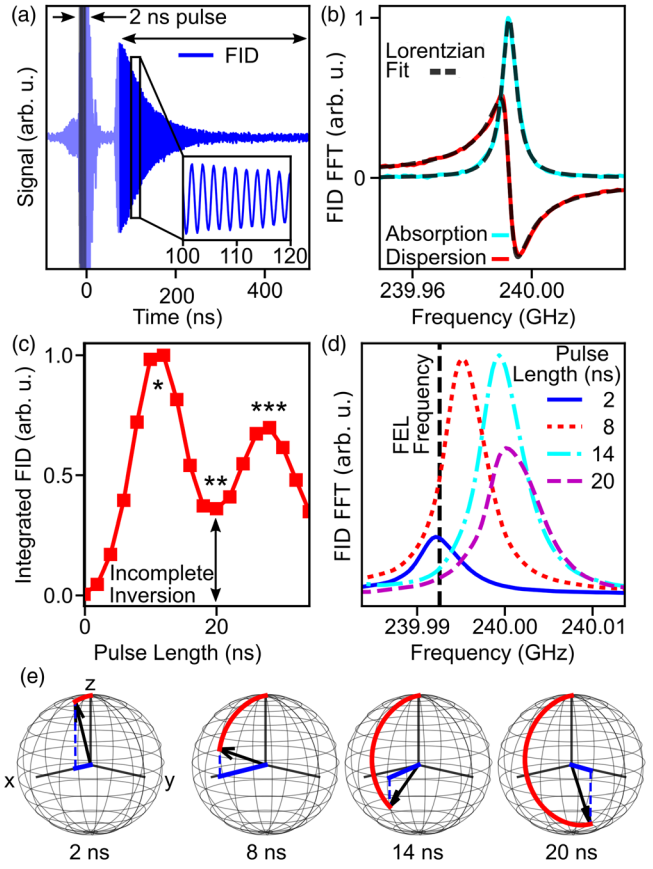

FIG. 1. (a) Room-temperature FID signal generated by a 2 ns FEL pulse, highlighted in gray, applied to a BDPA-Bz grain. Inset: signal digitized at the intermediate frequency (IF = 500 MHz, shown in inset). (b) Fourier transform of the FID generated by a 2 ns pulse. The FT-EPR line shape is well described by a Lorentzian with a FWHM of 5.9 ± 0.1 MHz. (c) Integrated FT-EPR intensity as a function of pulse length, demonstrating Rabi oscillations. The magnetic field was chosen so the FID generated by a 2 ns pulse is on resonance with the FEL pulse. For pulse lengths corresponding to the two maxima, the sample magnetization is rotated by $\pi/2$ (*) and by $3\pi/2$ (***), while at the minimum (**) the magnetization has been rotated by π. The minimum of the Rabi oscillation is not at zero, indicating incomplete population inversion. (d) FT-EPR absorption line shape plotted for four pulse lengths. The FID generated by a 2 ns pulse is on resonance with the FEL pulse; FIDs generated by longer pulses are not. (e) In red, the trajectory taken by the sample magnetization on the Bloch sphere. In blue, the magnetization vector projected onto the x-y plane.

where $\mathbf{H}_0 = \mathbf{B}_0/\mu_0$ is the externally applied magnetic field, $\gamma = g\mu_B/\hbar$ is the electron gyromagnetic ratio, and $\mathbf{M} \times \mathbf{M}$ identically vanishes.

Modeling the BDPA-Bz grain as an ellipsoid, the freely precessing magnetization $\mathbf{M}$ obeys the equations of motion

$$\frac{d}{dt}M_x = \mu_0\gamma(H_0 - (\delta_z - \delta_y)M_z)M_y - M_x/T_2, \tag{2a}$$

$$\frac{d}{dt}M_y = -\mu_0\gamma(H_0 - (\delta_z - \delta_x)M_z)M_x - M_y/T_2, \quad (2b)$$

$$\frac{d}{dt}M_z = \mu_0\gamma(\delta_x - \delta_y)M_xM_y - (M_z - M_0)/T_1, \quad (2c)$$

where δ_x, δ_x, δ_z are the principal values of N, M_0 is the equilibrium magnetization, and T_1 and T_2 are the phenomenological Bloch spin-spin and spin-lattice relaxation times [32]. Assuming axial symmetry so that $\delta_x = \delta_y = \delta_\perp$ and $\delta_z = \delta_\parallel$, the magnetization precesses at a frequency $\omega(M_z)$ which is a function of the z component of $\mathbf{M}$,

$$\omega(M_z) = \mu_0\gamma(H_0 - \theta_d M_z), \quad (3)$$

where $\theta_d = \delta_\parallel - \delta_\perp$. Two special cases are of particular interest: for a very thin, flat disk, $\theta_d = 1$, while for a sphere, $\theta_d = 0$ and the nonlinear term vanishes.

Equations (2) and (3) predict that the small tip-angle EPR frequency is shifted from the Larmor condition by an amount $\Delta\omega = -\mu_0\gamma\theta_d M_z$, neglecting higher order terms of order $|M_z^2/H_0|$. This is analogous to the FMR condition which appears in the Kittel equations [30]. However, unlike in the FMR case where changes in M_z due to resonant driving fields are negligible, for a paramagnet the full magnetization $\mathbf{M}$ can be rotated into the transverse plane or even inverted by a resonant microwave pulse, leading to a change in the precession frequency proportional to the change M_z. For BDPA-Bz, the maximum frequency shift, occurring when the initial room temperature magnetization $M_0 = M_{eq} = 270$ A/m [11] is inverted, can come to be $\Delta F \sim \theta_d \times 19$ MHz, which is on the order of the observed frequency shifts and several times the observed linewidth (Fig. 1).

A grain of BDPA-Bz with a geometry close to an axially symmetric ellipsoid [Fig. 2(a)], which had an aspect ratio of roughly 7:1 for $\theta_d = 0.65$, was selected for further experiments. Figure 2(b) shows a nutation experiment performed on this BDPA-Bz grain, with the colorbar indicating the FT-EPR signal strength and with the FT-EPR frequency indicated on the vertical axis. The magnetic field was chosen so the excitation pulses are resonant with the bare Larmor frequency, rather than with the small tip-angle frequency. As a consequence, the spin system initially has a precession frequency below the excitation frequency, but moves on to resonance for a $\pi/2$ pulse, moves to a frequency above the excitation frequency for a π pulse, and then returns to resonance for a $3\pi/2$ pulse. Rabi oscillations performed in this way achieve nearly complete magnetization inversion, as evidenced by the minimum being almost zero in Fig. 2(c).

Numerical simulations of the nonlinear modified Bloch equations with excitation pulses of varying lengths were carried out assuming an oblate spheroid geometry with an aspect ratio of 7:1, for an initial magnetization

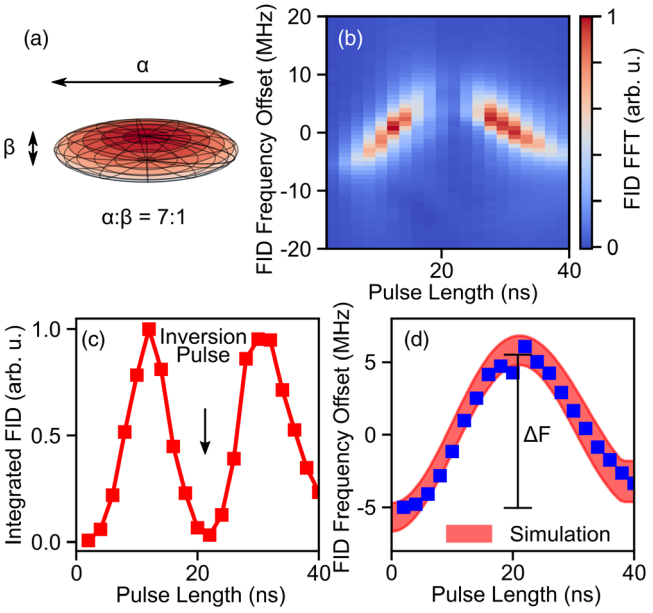

FIG. 2. (a) Schematic representation of a BDPA-Bz crystal as an oblate spheroid, with a ratio of major to semiminor axes of 7:1. (b) Contour plot of the FT-EPR absorption line shape, (c) integrated FID intensity, and (d) mean FID frequency, as a function of pulse length as BDPA-Bz magnetization undergoes Rabi oscillations. The FID frequency axes are referenced to the FEL frequency. The magnetic field is chosen so that the FID generated by a $\pi/2$ pulse has the same frequency as the FEL. The Rabi oscillations minimum is close to zero, indicating nearly complete population inversion is achieved with the magnetic field thus chosen.

$M_0 = 270$ A/m. The phenomenological Bloch relaxation times T_1 and T_2 were independently measured to be 270 ± 40 ns and 120 ± 30 ns, respectively, at 8.56 T (see Supplemental Material [33]), in good agreement with values measured at low field [13]. Simulations of the FID frequency dependence on pulse length over a full Rabi oscillation were in excellent agreement with experimental results, as shown in Fig. 2(d). The width of the simulated frequency shift indicates a 95% confidence interval, taking into account uncertainties in T_1, T_2, the Rabi frequency ω_1, and the FEL detuning (see Supplemental Material [33]).

Magnetization evolution was probed over many Rabi cycles by varying the pulse length from 0 to 700 ns in steps of 10 ns, using an on-resonance Rabi frequency $\omega_1/2\pi = 8$ MHz (Fig. 3). At least five Rabi cycles were observed. The width of the simulation indicates a 95% confidence interval and is in excellent agreement with experimental results. The decay in the observed Rabi oscillations is primarily related to spin-lattice (T_1) and spin-spin (T_2) relaxation.

The first condition for resolving a tip-angle dependent frequency shift in the dressed Rabi oscillation phase is that the ratio $|\Delta\omega/\Gamma| \geq 1$, where $\Delta\omega = -\mu_0\gamma\theta_d M_0$ is the demagnetizing field-induced frequency shift and Γ is the EPR linewidth. For BDPA-Bz grains at 8.56 T, $\Gamma \simeq 4$–6 MHz.

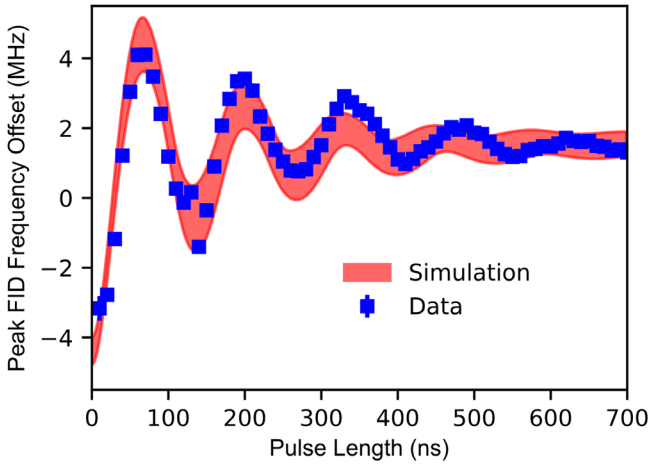

FIG. 3. Mean FID frequency as a function of pulse length as a BDPA-Bz crystal undergoes Rabi oscillations over many cycles. Simulated mean FID frequencies match experimental results over multiple oscillations.

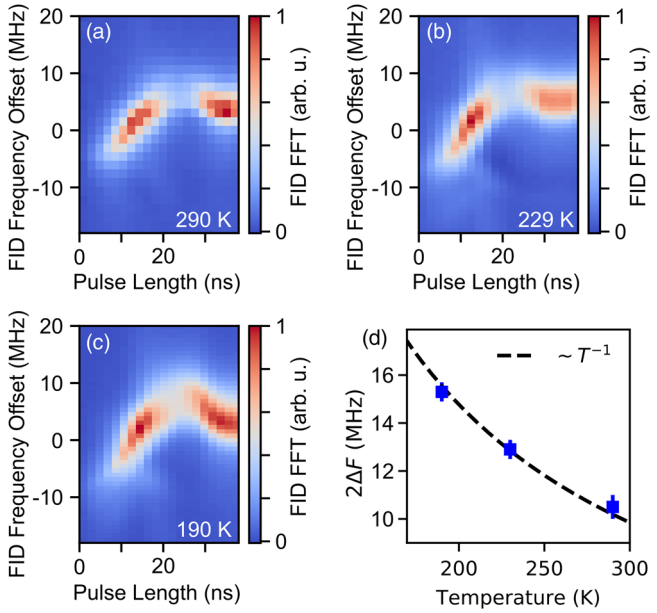

FIG. 4. Contour plots of the FT-EPR line shape at (a) 290 K, (b) 229 K, and (c) 190 K. (d) The maximum frequency shift ΔF as a function of temperature.

For $\theta_d = 0.65$ used in simulations described above, we have $|\Delta\omega/\Gamma| \simeq 1.3$. The second condition is that the ratio $\omega_1/\Gamma \geq 1$, where ω_1 is the Rabi frequency. For all previous EPR studies we are aware of, the combination of a sufficiently large equilibrium magnetization, narrow linewidth, and large Rabi frequency has been difficult to achieve, $|\Delta\omega/\Gamma| \ll 1$, and resolving magnetization-dependent frequency shifts has been difficult or impossible.

The temperature dependence of the fractional frequency shift $|\Delta\omega/\omega_L|$ in the dressed Rabi oscillation phase can be estimated for a paramagnet consisting of spin-1/2 electrons with density n at thermal equilibrium, where $M_0 = (g\mu_B/2)n\tanh(\mu_0\gamma H_0/2k_BT)$. When the high temperature approximation $k_BT \gg \mu_0\gamma\hbar H_0$ is valid,

$$\frac{\Delta\omega}{\omega_L} = \mu_0 n\frac{(\gamma\hbar)^2}{4k_BT}. \tag{4}$$

Figure 4 shows contour plots of nutation experiments performed at room temperature, 229 K, and 190 K. The temperature dependence of the maximum observed frequency shift ΔF is consistent with the predicted temperature dependence [Fig. 4(a)]. However, as the temperature is lowered, evidence of more complicated dynamics emerges in the nutation experiment: small additional frequency components are observed in FIDs for pulse durations shorter than 20 ns, as shown in Figs. 4(b) and 4(c).

Demagnetization field effects are commonly encountered in ferromagnetic resonance [30], where sample geometry plays an important role in determining the resonance condition at very small microwave fields and tip angles. However, as microwave fields are increased, even in spherical samples, spin wave instabilities destroy the state with spatially uniform magnetization before significant flip angles can be achieved [38]. Demagnetization field effects are also encountered in NMR in highly concentrated spin systems [39]. Nonlinear magnetization-dependent effects in NMR can manifest in the generation of multiple spin echos by a pair of radio frequency pulses [40–42] or in anomalous frequency correlations appearing in correlation spectroscopy experiments [43–45]. Taking $\theta_d = 1$, corresponding to a flat disk geometry, Eq. (4) predicts the ^{1}H NMR resonance measured in room-temperature water should shift by ~4 ppb, corresponding to a frequency shift of 1.6 Hz in a 9.4 T magnetic field. In 1990, Edzes reported an anomalous ^{1}H NMR frequency shift of ~2.5 ppb in protonated solvents, consistent with Eq. (4) for $\theta_d \sim 0.6$ [46]. Outside of this example, demagnetization field-induced frequency shifts are not commonly observed in NMR, which can be explained by the fact that the gyromagnetic ratio of electrons is 657 times larger than that of protons, together with the γ^2 dependence of Eq. (4).

Another nonlinear, magnetization-dependent effect encountered in magnetic resonance experiments is radiation damping [47]. Radiation damping typically manifests as magnetization and tip-angle dependent line broadening [48] in magnetic resonance experiments which employ resonators with $Q \gg 1$, with high filling factors [49,50]. The effects of radiation damping are small in our experiments, since we do not employ a resonator cavity and our effective filling factor $\eta \ll 1$, but may be responsible for some line broadening (see Supplemental Material [33]).

Direct radiative losses due to magnetic dipole radiation may also contribute to the observed EPR linewidths, especially at low temperatures. The instantaneous power P radiated by magnetic dipole radiation at frequency ω by a sample of volume V with uniform magnetization M_0 is given by $P = (\mu_0/6\pi c^3)\omega^4 M_0^2 V^2 \sin^2\theta$, where θ is the

magnetization tip angle. Radiative losses lead to magnetization decay with characteristic time constant $\tau_{\mathrm{rad}} = [(\mu_0/6\pi c^3)\gamma\omega^3 M_0 V]^{-1}$ (see Supplemental Material [33]). For the grain used in experiments presented in Fig. 2, a lower limit of $\tau_{\mathrm{rad}} \simeq 360$ ns was calculated, which is longer than T_2, $T_2^* = 1/\pi\Gamma$, or T_1, but which may become important to the linewidth at low temperatures.

Nonlinear spin-spin interactions like those reported in this Letter are essential for developing the quantum-mechanical correlations between spins necessary to generate squeezed spin states [51]. Schemes for realizing squeezed states of electron spin ensembles have been proposed involving phonon-induced interactions between nitrogen-vacancy (NV) centers in diamond [52], or by coupling a NV center ensemble to a magnetic tip attached to a nanomechanical resonator [53]. Demagnetization field effects offer an alternative method of engineering nonlinear spin-spin interactions. The nonlinear interaction strength can be tuned by optimizing the sample geometry, as illustrated by Eq. (2). The long-range magnetic interactions that dress Rabi oscillations in this work may also be useful for coupling distant spin qubits [54].

In this Letter, we have shown that, when both the microwave field and the demagnetization field are larger than the linewidth of a magnetic resonance, the noninteracting spin dynamics may be visibly "dressed" by each spin's interaction with the mean field generated by all the other spins in the sample. The signatures of dressed Rabi oscillations are free-induction decays whose frequencies depend on tip angle, and anomalous noncircular trajectories of the sample magnetization direction on the surface of the Bloch sphere. We think of dressed Rabi oscillation as a transient dynamical phase in a system of interacting spins driven far from thermal equilibrium. Dressed Rabi oscillation can be modeled using classical equations of motion. As the temperature is lowered, in addition to the strength of the dressing increasing, the thermal fluctuations in the exchange fields that are responsible for narrowing the EPR line near room temperature will be quenched, and signatures of new manifestly quantum states of interacting spins far from thermal equilibrium may emerge.

The authors acknowledge David Enyeart and Nickolay Agladze for maintaining, repairing, and assisting with operation of the UCSB FEL, and Gerald Ramian for many useful discussions. Support for this work came from the National Science Foundation through NSF-MCB-1617025. This work was performed at the ITST Terahertz Facilities at UCSB, which have been upgraded with funds from NSF-DMR-1126894 and NSF-DMR-1626681.

*Corresponding author.
sherwin@physics.ucsb.edu

[1] P. Anderson, Mater. Res. Bull. **8**, 153 (1973).
[2] T. Senthil and M. P. A. Fisher, Phys. Rev. B **62**, 7850 (2000).
[3] R. Moessner and S. L. Sondhi, Phys. Rev. Lett. **86**, 1881 (2001).
[4] A. Kitaev, Ann. Phys. (Amsterdam) **321**, 2 (2006).
[5] L. Balents, Nature (London) **464**, 199 (2010).
[6] B. J. Powell and R. H. McKenzie, Rep. Prog. Phys. **74**, 056501 (2011).
[7] L. Savary and L. Balents, Rep. Prog. Phys. **80**, 016502 (2016).
[8] M. Vojta, Rep. Prog. Phys. **81**, 064501 (2018).
[9] D. V. Else, B. Bauer, and C. Nayak, Phys. Rev. Lett. **117**, 090402 (2016).
[10] S. Choi, J. Choi, R. Landig, G. Kucsko, H. Zhou, J. Isoya, F. Jelezko, S. Onoda, H. Sumiya, V. Khemani *et al.*, Nature (London) **543**, 221 (2017).
[11] W. Duffy, J. F. Dubach, P. A. Pianetta, J. F. Deck, D. L. Strandburg, and A. R. Miedema, J. Chem. Phys. **56**, 2555 (1972).
[12] N. Azuma, T. Ozawa, and J. Yamauchi, Bull. Chem. Soc. Jpn. **67**, 31 (1994).
[13] D. G. Mitchell, R. W. Quine, M. Tseitlin, R. T. Weber, V. Meyer, A. Avery, S. S. Eaton, and G. R. Eaton, J. Phys. Chem. B **115**, 7986 (2011).
[14] J. Yamauchi and Y. Deguchi, Bull. Chem. Soc. Jpn. **50**, 2803 (1977).
[15] W. O. Hamilton and G. E. Pake, J. Chem. Phys. **39**, 2694 (1963).
[16] M. Bennati, C. Farrar, J. Bryant, S. Inati, V. Weis, G. Gerfen, P. Riggs-Gelasco, J. Stubbe, and R. Griffin, J. Magn. Reson. **138**, 232 (1999).
[17] D. Goldfarb, Y. Lipkin, A. Potapov, Y. Gorodetsky, B. Epel, A. M. Raitsimring, M. Radoul, and I. Kaminker, J. Magn. Reson. **194**, 8 (2008).
[18] C. Durkan and M. E. Welland, Appl. Phys. Lett. **80**, 458 (2002).
[19] E. L. Dane and T. M. Swager, J. Org. Chem. **75**, 3533 (2010).
[20] P. Giraudeau, Y. Shrot, and L. Frydman, J. Am. Chem. Soc. **131**, 13902 (2009).
[21] P. W. Anderson and P. R. Weiss, Rev. Mod. Phys. **25**, 269 (1953).
[22] S. K. Misra, *Multifrequency Electron Paramagnetic Resonance: Theory and Applications* (John Wiley and Sons, Hoboken, NJ, 2011).
[23] F. A. Hegmann and M. S. Sherwin (International Society for Optics and Photonics, 1996) pp. 90–106.
[24] S. Takahashi, G. Ramian, and M. S. Sherwin, Appl. Phys. Lett. **95**, 234102 (2009).
[25] S. Takahashi, G. Ramian, M. S. Sherwin, L.-C. Brunel, and J. van Tol, Appl. Phys. Lett. **91**, 174102 (2007).
[26] S. Takahashi, L. C. Brunel, D. T. Edwards, J. van Tol, G. Ramian, S. Han, and M. S. Sherwin, Nature (London) **489**, 409 (2012).
[27] D. T. Edwards, Y. Zhang, S. J. Glaser, S. Han, and M. S. Sherwin, Phys. Chem. Chem. Phys. **15**, 5707 (2013).
[28] C. B. Wilson, S. Aronson, J. A. Clayton, S. J. Glaser, S. Han, and M. S. Sherwin, Phys. Chem. Chem. Phys. **20**, 18097 (2018).
[29] I. I. Rabi, Phys. Rev. **51**, 652 (1937).
[30] C. Kittel, Phys. Rev. **73**, 155 (1948).
[31] A. Zangwill, *Modern Electrodynamics*, 1st ed. (Cambridge University Press, Cambridge, 2013).

[32] F. Bloch, Phys. Rev. **70**, 460 (1946).
[33] See Supplemental Material at http://link.aps.org/supplemental/10.1103/PhysRevLett.124.047201, which includes Refs. [34–37], for details on temperature dependence, on detuning dependence, on measurements of relaxation times, and on numerical simulations.
[34] J. R. Klauder and P. W. Anderson, Phys. Rev. **125**, 912 (1962).
[35] K. Salikhov, S. Dzuba, and A. Raitsimring, J. Magn. Reson. (1969) **42**, 255 (1981).
[36] A. Schweiger and G. Jeschke, *Principles of Pulse Electron Paramagnetic Resonance* (Oxford University Press, Oxford, 2001).
[37] S. Bloom, J. Appl. Phys. **28**, 800 (1957).
[38] H. Suhl, Proc. IRE **44**, 1270 (1956).
[39] M. H. Levitt, Concepts Magn. Reson. **8**, 77 (1996).
[40] R. Bowtell, R. Bowley, and P. Glover, J. Magn. Reson. **88**, 643 (1990).
[41] G. Deville, M. Bernier, and J. M. Delrieux, Phys. Rev. B **19**, 5666 (1979).
[42] A. Bedford, R. Bowtell, and R. Bowley, J. Magn. Reson. (1969) **93**, 516 (1991).
[43] W. Warren, W. Richter, A. Andreotti, and B. Farmer, Science **262**, 2005 (1993).
[44] W. Richter, S. Lee, W. Warren, and Q. He, Science **267**, 654 (1995).
[45] J. Jeener, J. Chem. Phys. **112**, 5091 (2000).
[46] H. T. Edzes, J. Magn. Reson. (1969) **86**, 293 (1990).
[47] N. Bloembergen and R. V. Pound, Phys. Rev. **95**, 8 (1954).
[48] M. Augustine, Prog. Nucl. Magn. Reson. Spectrosc. **40**, 111 (2002),
[49] H. Benner, J. Appl. Phys. **13**, 141 (1977).
[50] T. Prisner, S. Un, and R. Griffin, Isr. J. Chem. **32**, 357 (1992).
[51] M. Kitagawa and M. Ueda, Phys. Rev. A **47**, 5138 (1993).
[52] S. D. Bennett, N. Y. Yao, J. Otterbach, P. Zoller, P. Rabl, and M. D. Lukin, Phys. Rev. Lett. **110**, 156402 (2013).
[53] Y.-H. Ma, X.-F. Zhang, J. Song, and E. Wu, Ann. Phys. (Amsterdam) **369**, 36 (2016).
[54] L. Trifunovic, F. L. Pedrocchi, and D. Loss, Phys. Rev. X **3**, 041023 (2013).